6G mURLLC over Cell-Free Massive MIMO Systems in the Finite Blocklength Regime

Zhong Li[1(✉)], Jie Zeng[2], Wen Zhang[1], Shidong Zhou[2], and Ren Ping Liu[3]

[1] School of Communication and Information Engineering, Chongqing University of Posts and Telecommunications, Chongqing 400065, China
{s190131188,s190131003}@stu.cqupt.edu.cn
[2] Department of Electronic Engineering, Tsinghua University, Beijing 100084, China
{zengjie,zhousd}@tsinghua.edu.cn
[3] School of Electrical and Data Engineering, University of Technology Sydney, Sydney 2007, Australia
RenPing.Liu@uts.edu.au

Abstract. In order to support the new service requirements-massive ultra-reliable low-latency communications (mURLLC) in the six-generation (6G) mobile communication system, finite blocklength (FBL) information theory has been introduced. Furthermore, cell-free massive multiple input multiple output (MIMO) has emerged as one of the 6G essential promising technologies. A great quantity of distributed access points (APs) jointly serve massive user equipment (UE) at the same time-frequency resources, which can significantly improve various quality-of-service (QoS) metrics for supporting mURLLC. However, as the number of UE grows, the orthogonal pilot resources in the coherent time are insufficient. This leads to serious non-orthogonal pilot contamination and pilot allocation imbalance. Therefore, we propose an analytical cell-free massive MIMO system model and precisely characterize the error probability metric. In particular, we propose a FBL based system model, formulate and resolve the error probability minimization problem, given the latency requirement. Simulation results verify the effectiveness of the proposed scheme and show that the error probability can be improved by up to 15.9%, compared with the classic pilot allocation scheme.

Keywords: Cell-free massive multiple input multiple output (MIMO) · Finite blocklength (FBL) · mURLLC · Pilot allocation

1 Introduction

With the rapid expansion of wireless communication systems, the amount of mobile users has shown an explosive trend. The growth of mobile users has

Supported by the National Key R&D Program (No. 2018YFB1801102), the Natural Science Foundation of Beijing (No. L192025), the National Natural Science Foundation of China (No. 62001264), and the China Postdoctoral Science Foundation (No. 2020M680559 and No. 2021T140390).

H. Gao et al. (Eds.): ChinaCom 2021, LNICST 433, pp. 425–437, 2022.
https://doi.org/10.1007/978-3-030-99200-2_32

benefited from the popularization of smart terminals and the emergence of various new mobile services. However, due to multiple constraints such as energy, spectral efficiency, and cost, the current fifth-generation (5G) mobile communication system cannot meet the requirements for ultra-large traffic, ultra-low latency, ultra-large connections, and ultra-high reliability. Therefore, the sixth-generation (6G) mobile communication system is regarded as the future research focus.

Although it is far from reaching the unified stage of 6G definition, based on the research progress [1–4] of various countries, it can be predicted that 6G will adopt transformative technologies from the cell-free network architecture [5,6].

As we all know, the cellular network architecture is an epoch-making concept proposed by Bell Labs in the 1970s. It adopts frequency reuse and cell splitting technologies to improve the exploitation of spectrum resources and support the rapid development of mobile communications. In order to satisfy the ever-increasing requirements for services, the entire evolution of mobile communication systems from the first-generation (1G) mobile communication system to 5G is based on cellular networks, that is, using macro cell splitting and vertical micro cell network layering. However, as the cell area continues to shrink, problems such as inter-cell interference and frequent handovers have become more and more serious, resulting in a bottleneck in system performance improvement. In order to overcome these challenges, a cell-free massive multiple input multiple output (MIMO) network architecture [7] which completely reforms the cellular network architecture has become one of the feasible solutions.

The cell-free massive MIMO system distributes a great quantity of access points (APs) with one or more antennas in a wide area, transmits data to the central processing unit (CPU) through the backhaul links, and serves massive user equipment (UE) at the same time-frequency resources. Cell-free massive MIMO combines the advantages of distributed antenna systems and centralized massive MIMO, that is, introducing the idea of "user-centric" [7,8]. It can reduce the distances between APs and UE, obtain spatial macro diversity gain, greatly cut down the path loss, and use the favorable propagation brought by a great quantity of APs to reduce the interference among massive users, so that the entire area is covered evenly and the user experience is significantly improved [8]. Due to these advantages, cell-free massive MIMO is very suitable for major hospitals, stadiums, high-speed rail stations, office buildings, shopping malls and other hot spot scenes, and is considered to be one of the important research directions in future mobile communication systems.

Since the amount of users rapidly increases, the orthogonal pilot resources in the coherent time are insufficient, which leads to serious non-orthogonal pilot contamination and pilot allocation imbalance. The authors of [9] designed random and structured non-orthogonal pilot allocation schemes to maximize the user pilot reuse distance. In [10], the authors used a dynamic pilot multiplexing method to make two users share the same pilot resource to maximize the uplink sum rate. Literature [11] divided users into groups based on available pilot resources, and assigned a pilot sequence to each user group, but there was still

pilot contamination among user groups. Moreover, the authors of [12] proposed random and orthogonal pilot allocation schemes, but there was a large waste of resources.

In addition, since the wireless fading channels has the stochastic nature, it is difficult to satisfy the requirements for ultra-reliable low-latency communications (URLLC). Moreover, as one promising technique for supporting latency-sensitive services, massive ultra-reliable and low-latency communications (mURLLC) combines URLLC with massive access. Meanwhile, massive short-packet data transmissions are required in mURLLC to support latency-sensitive applications [13]. This indicates that the classical Shannon theory with infinite blocklength coding is not applicable to the new scenario any more. Therefore, finite blocklength (FBL) information theory [14] has been developed to satisfy both ultra-reliable and low-latency requirements by short-packet data transmissions. Therefore, we analyze the error probability performance over 6G cell-free massive MIMO systems and optimize the pilot length to minimize the error probability.

The remainder of this paper is organized as follows. Section 2 describes the cell-free massive MIMO system model. Section 3 formulates the downlink error probability minimization and presents the golden section search algorithm for the pilot optimization problem. Section 4 presents the simulation and numerical results. Finally, Sect. 5 concludes this paper.

2 System Model

Take into consideration a cell-free massive MIMO system which consists of one CPU, K APs and M UE, as shown in Fig. 1. M UE are served by K APs at the same time-frequency resources. It is assumed that the APs and UE are located randomly in a wide area. Assume that each AP has N antennas, while each UE has a single antenna. Moreover, all APs are linked to a CPU through infinite perfect backhaul links. Furthermore, we assume that the system is operated under time-division duplexing (TDD) mode, which can permit channel reciprocity to require the downlink channel state information (CSI) by uplink pilot training. In addition, we let n_{p} represent the number of channel uses for uplink pilot training, n_{d} for downlink data transmission, and n for the whole transmission, i.e., $n = n_{\mathrm{p}} + n_{\mathrm{d}}$. The channel coefficient between the kth AP (AP-k) and the mth UE (UE-m), denoted by $\boldsymbol{g}_{k,m} \in \mathbb{C}^{N\times 1}$, can be characterized as

$$\boldsymbol{g}_{k,m} = \boldsymbol{h}_{k,m}\sqrt{\beta_{k,m}} \tag{1}$$

where $\beta_{k,m}$ denotes the large-scale fading coefficient and $\boldsymbol{h}_{k,m}$ denotes the small-scale vector.

2.1 Uplink Pilot Training

The pilot training sequence for UE-m is defined as $\boldsymbol{\varphi}_m^{n_{\mathrm{p}}} = \left[\varphi_m^{(1)}, \ldots, \varphi_m^{(n_{\mathrm{p}})}\right] \in \mathbb{C}^{1\times n_{\mathrm{p}}}$ and $\left\|\boldsymbol{\varphi}_m^{n_{\mathrm{p}}}\right\|^2 = 1$ where $\|\cdot\|$ represents the Euclidean norm. Therefore, the received signal at AP-k, denoted by $\mathbf{Y}_k^{n_{\mathrm{p}}} \in \mathbb{C}^{N\times n_{\mathrm{p}}}$, is derived as

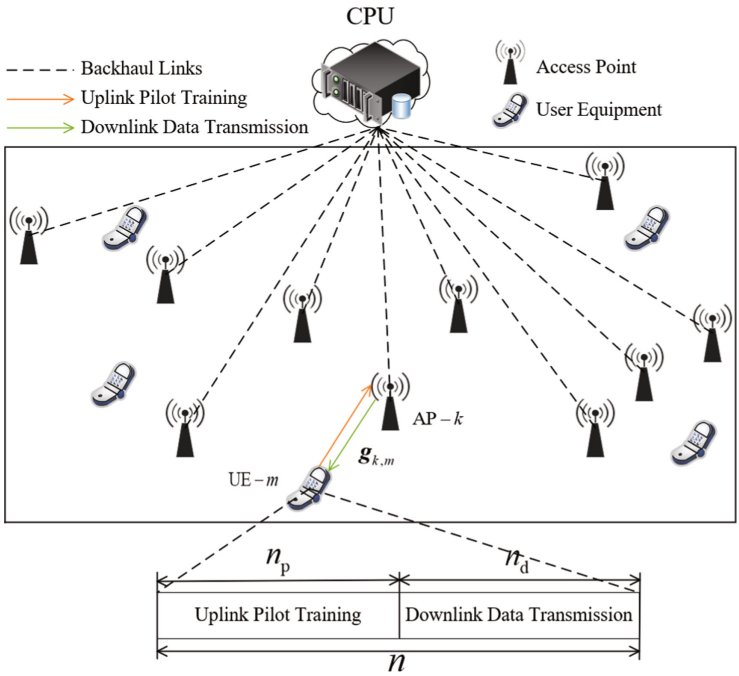

Fig. 1. The cell-free massive MIMO system model.

$$\mathbf{Y}_k^{n_\mathrm{p}} = \sqrt{n_\mathrm{p}\mathcal{P}_\mathrm{p}} \sum_{m=1}^{M} \boldsymbol{g}_{k,m} \boldsymbol{\varphi}_m^{n_\mathrm{p}} + \mathbf{N}_k \tag{2}$$

where $\mathcal{P}_\mathrm{p}$ denotes the pilot transmit power at the UE and $\mathbf{N}_k \in \mathbb{C}^{N \times n_\mathrm{p}}$ denotes the additive white Gaussian noise (AWGN) matrix with zero mean and covariance $\mathbf{I}_N$, where $\mathbf{I}_N$ denotes the identity matrix with size N.

The projection of $\mathbf{Y}_k^{n_\mathrm{p}}$ onto $\boldsymbol{\varphi}_m^{n_\mathrm{p}}$, denoted by $\boldsymbol{y}_{k,m}^{n_\mathrm{p}} \in \mathbb{C}^{N \times 1}$, can be derived as

$$\boldsymbol{y}_{k,m}^{n_\mathrm{p}} = \mathbf{Y}_k^{n_\mathrm{p}} \left(\boldsymbol{\varphi}_m^{n_\mathrm{p}}\right)^H = \sqrt{n_\mathrm{p}\mathcal{P}_\mathrm{p}} \boldsymbol{g}_{k,m} + \sum_{\substack{m'=1 \\ m' \neq m}}^{M} \sqrt{n_\mathrm{p}\mathcal{P}_\mathrm{p}} \boldsymbol{g}_{k,m'} + \boldsymbol{n}_k, \tag{3}$$

where $(\cdot)^H$ denotes the conjugate transpose and $\boldsymbol{n}_k \triangleq \mathbf{N}_k \left(\boldsymbol{\varphi}_m^{n_\mathrm{p}}\right)^H \in \mathbb{C}^{N \times 1}$ is an independent and identically distributed (i.i.d.) Gaussian vector with zero mean and covariance $\mathbf{I}_N$.

Denote $\mathbf{G}_k \triangleq \left[\boldsymbol{g}_{k,1}, \ldots, \boldsymbol{g}_{k,M}\right]$ as the channel coefficient matrix from the AP-k to all UEs. Furthermore, we denote $\mathbf{R}_{\mathbf{G}_k} \triangleq \mathbb{E}\left[\mathbf{G}_k \left(\mathbf{G}_k\right)^H\right] = \mathrm{diag}\left(\beta_{k,1}, \ldots, \beta_{k,M}\right)$ as the covariance matrix of $\mathbf{G}_k$, where $\mathbb{E}[\cdot]$ represents the

expectation operation and diag(·) denotes the diagonal matrix. Then, the minimum mean-squared error (MMSE) estimator which is represented by $\widehat{\mathbf{G}}_k$, is given by [15]

$$\widehat{\mathbf{G}}_k = \sqrt{n_{\mathrm{p}}\mathcal{P}_{\mathrm{p}}}\mathbf{R}_{\mathbf{G}_k}\left(n_{\mathrm{p}}\mathcal{P}_{\mathrm{p}}\mathbf{R}_{\mathbf{G}_k} + \mathbf{I}_N\right)^{-1}\boldsymbol{y}_{k,m}^{n_{\mathrm{p}}}. \tag{4}$$

Furthermore, the channel estimator $\hat{\boldsymbol{g}}_{k,m}$ is derived as

$$\hat{\boldsymbol{g}}_{k,m} = \frac{\sqrt{n_{\mathrm{p}}\mathcal{P}_{\mathrm{p}}}\beta_{k,m}}{n_{\mathrm{p}}\mathcal{P}_{\mathrm{p}}\sum_{m'=1}^{M}\beta_{k,m'}\left|\boldsymbol{\varphi}_m\left(\boldsymbol{\varphi}_{m'}\right)^H\right|^2 + 1}\boldsymbol{y}_{k,m}^{n_{\mathrm{p}}}. \tag{5}$$

It is noted that the channel estimator $\hat{\boldsymbol{g}}_{k,m}$ consists of N independent elements. The variance of each element of $\hat{\boldsymbol{g}}_{k,m}$ is given by

$$\sigma_{k,m} = \frac{n_{\mathrm{p}}\mathcal{P}_{\mathrm{p}}\beta_{k,m}^2}{n_{\mathrm{p}}\mathcal{P}_{\mathrm{p}}\sum_{m'=1}^{M}\beta_{k,m'}\left|\boldsymbol{\varphi}_m\left(\boldsymbol{\varphi}_{m'}\right)^H\right|^2 + 1}. \tag{6}$$

The MMSE estimation error is $\widetilde{\boldsymbol{g}}_{k,m} = \boldsymbol{g}_{k,m} - \hat{\boldsymbol{g}}_{k,m}$, which is independent of the true channel. Moreover, each element of the channel estimate error follows $\mathcal{CN}\left(0, \beta_{k,m} - \gamma_{k,m}\right)$.

2.2 Downlink FBL Data Transmission

We let Q_m denote the multiplexing order of UE-m. Furthermore, we define a Q_m-dimensional beamformer $\mathbf{B}_m \triangleq \mathbf{I}_{Q_m} \otimes \mathbf{1}_{N/Q_m}$ for UE-m, where $\otimes$ represents the Kronecker product, $\mathbf{I}_{Q_m}$ represents the identity matrix with size Q_m, and $\mathbf{1}_{N/Q_m}$ represents the all one vector with size N/Q_m. Denote $\mathbf{X}_k^{n_{\mathrm{d}}} \triangleq \left[\boldsymbol{x}_k^{(1)}, \ldots, \boldsymbol{x}_k^{(n_{\mathrm{d}})}\right]$ as the transmitted signal matrix from AP-k and $\boldsymbol{y}_m^{n_{\mathrm{d}}} \triangleq \left[y_m^{(1)}, \ldots, y_m^{(n_{\mathrm{d}})}\right]$ as the received signal vector at UE-m. Based on the MMSE estimator matrix which is represented by $\widehat{\mathbf{G}}_k = \left[\widehat{\boldsymbol{g}}_{k,1}, \ldots, \widehat{\boldsymbol{g}}_{k,M}\right]$, the transmitted signal which is represented by $\mathbf{x}_k^{(l)}$, for transmitting lth data block by using conjugate beamforming [7], is derived as

$$\boldsymbol{x}_k^{(l)} = \mathbf{W}_k\left(\boldsymbol{\Sigma}_k\right)^{\frac{1}{2}} s_m^{(l)}, \quad l = 1, \ldots, n_{\mathrm{d}} \tag{7}$$

where $s_m^{(l)}$ is the lth data block to UE-m. $\boldsymbol{\Sigma}_k \triangleq \mathrm{diag}\left(\eta_{k,1}, \ldots, \eta_{k,M}\right)$ represents the power coefficient matrix where $\eta_{k,m}(m = 1, \ldots, M)$ represents the power coefficient for transmitting lth data block from AP-k to UE-m. $\mathbf{W}_k$ represents the downlink precoder, which is given by

$$\mathbf{W}_k \triangleq \widehat{\mathbf{G}}_k\left[\left(\widehat{\mathbf{G}}_k\right)^H\widehat{\mathbf{G}}_k\right]^{-1}\mathbf{B}_m\left(\boldsymbol{\Xi}_k\right)^{\frac{1}{2}} \tag{8}$$

where $\boldsymbol{\Xi}_k = \mathrm{diag}\left(\chi_1, \ldots, \chi_M\right)$ represents the normalization matrix. Therefore, the columns of $\mathbf{W}_k$ have unit norm and the normalization variable $\chi_k(k = 1, \ldots, M)$ which are following the central chi-square distribution with

(2ℓ) degrees of freedom, where $\ell = K - M + 1$. The probability density function (PDF) of χ_k is given by [16]

$$f_\ell(\chi_k) = \frac{1}{\Gamma(\ell)} \chi_k^{\ell-1} e^{-\chi_k} \tag{9}$$

where $\Gamma(z) = \int_0^{+\infty} t^{z-1} e^{-t} dt$ represents the Gamma function. Define $\mathbf{W}_k = [\boldsymbol{w}_{k,1}, \ldots, \boldsymbol{w}_{k,M}]$ where $\boldsymbol{w}_{k,m}$ represents the downlink precoder. Furthermore, the power constraint at each AP on power coefficients is given by

$$\frac{1}{n_\mathrm{d}} \sum_{l=1}^{n_\mathrm{d}} \mathbb{E}\left[\left\|\boldsymbol{x}_k^{(l)}\right\|^2\right] \leq \overline{\mathcal{P}}_\mathrm{d} \tag{10}$$

where $\overline{\mathcal{P}}_\mathrm{d}$ denotes the average transmit power for each AP and $\boldsymbol{x}_k^{(l)}$ is derived by (7). In addition, with the number of APs K growing, the system will experience only small variations (with respect to the average) in the achievable data rate, which is known as the channel hardening [17]. Then, although the instantaneous CSI is not available at the UE, $\mathbb{E}\left[\left(\boldsymbol{g}_{k,m}\right)^T \boldsymbol{w}_{k,m}\right]$ can be used to calculate the channel coefficient, where $(\cdot)^T$ represents the transpose of a vector.

The received signal, denoted by $y_m^{(l)}$, for transmitting the lth finite-blocklength data block from AP-k to UE-m, is derived as

$$\begin{aligned} y_m^{(l)} = & \underbrace{\sum_{k=1}^{K} \sqrt{\overline{\mathcal{P}}_\mathrm{d} \eta_{k,m}} \mathbb{E}\left[\left(\boldsymbol{g}_{k,m}\right)^T \boldsymbol{w}_{k,m}\right] s_m^{(l)}}_{\mathrm{DS}_m} \\ & + \underbrace{\sqrt{\overline{\mathcal{P}}_\mathrm{d}} \left\{\sum_{k=1}^{K} \sqrt{\eta_{k,m}} \left(\boldsymbol{g}_{k,m}\right)^T \boldsymbol{w}_{k,m} - \mathbb{E}\left[\sum_{k=1}^{K} \sqrt{\eta_{k,m}} \left(\boldsymbol{g}_{k,m}\right)^T \boldsymbol{w}_{k,m}\right]\right\} s_m^{(l)}}_{\mathrm{BU}_m} \\ & + \sum_{\substack{m'=1 \\ m' \neq m}}^{M} \underbrace{\sum_{k=1}^{K} \sqrt{\overline{\mathcal{P}}_\mathrm{d} \eta_{k,m'}} \left(\boldsymbol{g}_{k,m}\right)^T \boldsymbol{w}_{k,m'} s_{m'}^{(l)}}_{\mathrm{UI}_{m'}} + n_m^{(l)} \end{aligned} \tag{11}$$

where $s_m^{(l)}$ and $s_{m'}^{(l)}$ represent the signals sent to UE-m and UE-m', respectively; $\eta_{k,m}$ and $\eta_{k,m'}$ represent the power coefficients for UE-m and UE-m', respectively; $\boldsymbol{g}_{k,m} \in \mathbb{C}^{1\times N}$ represents the channel coefficient vector from AP-k to UE-m; $n_m^{(l)}$ represents the AWGN; and DS_m, BU_m, and $\mathrm{UI}_{m'}$ are the strength of the desired signal, the beamforming gain uncertainty, and the interference caused by UE-m', respectively.

Correspondingly, the signal to noise plus interference ratio (SINR) which is represented by γ_m, from the APs to UE-m, is derived by

$$\gamma_m = \frac{\|\mathrm{DS}_m\|^2}{\mathbb{E}\left[\|\mathrm{BU}_m\|^2\right] + \sum_{\substack{m'=1 \\ m' \neq m}}^{M} \mathbb{E}\left[\|\mathrm{UI}_{m'}\|^2\right] + 1} \tag{12}$$

3 Minimize the Error Probability in the FBL Regime

In the FBL regime, the accurate approximation of the achievable data rate for UE-m, denoted by R_m (bits per channel use), with error probability, denoted by $\epsilon_m (0 \leq \epsilon_m < 1)$, and coding blocklength, denoted by n_{d}, is given by [14]

$$R_m \left(n_{\mathrm{d}}, \epsilon_m\right) \approx C\left(\gamma_m\right) - \sqrt{\frac{V\left(\gamma_m\right)}{n_{\mathrm{d}}}} Q^{-1}\left(\epsilon_m\right) \tag{13}$$

where $Q(x) = \int_x^{+\infty} \frac{1}{\sqrt{2\pi}} e^{-\frac{1}{2}t^2} dt$ denotes the Q-function and $Q^{-1}(\cdot)$ denotes the inverse of Q-function. $C(\gamma_m)$ and $V(\gamma_m)$ represent the channel capacity and channel dispersion, respectively, which are given by [14]

$$\begin{cases} C\left(\gamma_m\right) = \log_2\left(1 + \gamma_m\right) \\ V\left(\gamma_m\right) = 1 - \frac{1}{\left(1+\gamma_m\right)^2} \end{cases} \tag{14}$$

Since $n = Bt_{\mathrm{D}} = n_{\mathrm{p}} + n_{\mathrm{d}}$ where B denotes the bandwidth and t_{D} denotes the latency, the achievable data rate R_m for UE-m, given the pilot length n_{p}, is given by

$$R_m \left(t_{\mathrm{D}}, \epsilon_m\right) \approx C\left(\gamma_m\right) - \sqrt{\frac{V\left(\gamma_m\right)}{Bt_{\mathrm{D}} - n_{\mathrm{p}}}} Q^{-1}\left(\epsilon_m\right). \tag{15}$$

In the case where the achievable data rates for all UE are given, i.e., $R_m = \frac{D}{Bt_{\mathrm{D}} - n_{\mathrm{p}}} (m = 1, \ldots, M)$, where D is the size of downlink data packet (measured in bits). The error probability for UE-m can be derived as

$$\epsilon_m \left(t_{\mathrm{D}}, n_{\mathrm{p}}\right) \approx Q\left(\sqrt{\frac{Bt_{\mathrm{D}} - n_{\mathrm{p}}}{V\left(\gamma_m\right)}} \left[C\left(\gamma_m\right) - \frac{D}{Bt_{\mathrm{D}} - n_{\mathrm{p}}}\right]\right) \tag{16}$$

Given the latency which can satisfy mURLLC ($t_{\mathrm{D}} \leq 0.5$ ms), the error probability is a function of the pilot length n_{p}. Therefore, the optimization problem to minimize the error probability can be modeled as

$$n_{\mathrm{p}}^* = \underset{M \leq n_{\mathrm{p}} \leq Bt_{\mathrm{D}} - 1}{\arg\min} \epsilon_m \left(n_{\mathrm{p}}\right). \tag{17}$$

In order to find the optimal pilot length n_{p}^*, the exhaustive method is often used. However, the low-complexity golden section search algorithm can be used as an effective solution to quickly converge to the optimal pilot length to reduce computational complexity. The detailed steps of the golden section search algorithm are listed in Algorithm 1.

The complexity of the golden section search algorithm is $\mathcal{O}(log(Bt_{\mathrm{D}} - K))$, which is much lower than the complexity of the exhaustive method $\mathcal{O}(Bt_{\mathrm{D}} - K)$.

Algorithm 1. Golden section search algorithm

Input: Number of UE M, bandwidth B, latency t_{D}
Initialization: Search interval $[n_{\mathrm{L}}, n_{\mathrm{R}}]$, $n_{\mathrm{L}} = M$, $n_{\mathrm{R}} = Bt_{\mathrm{D}} - 1$, tolerance $t_{\mathrm{tol}} = 0.5$, golden ratio $\rho = 0.618$
do
  $n_1 = n_{\mathrm{L}} + (1+\rho)(n_{\mathrm{R}} - n_{\mathrm{L}})$ and $n_2 = n_{\mathrm{L}} + \rho(n_{\mathrm{R}} - n_{\mathrm{L}})$
  Calculate the error probability $\epsilon_k(n_1)$ and $\epsilon_k(n_2)$
  if $\epsilon_k(n_1) < \epsilon_k(n_2)$ **then**
    $n_{\mathrm{R}} = n_2$, $n_2 = n_1$, and $n_1 = n_{\mathrm{D}} + (1-\rho)(n_{\mathrm{R}} - n_{\mathrm{L}})$
  else
    $n_{\mathrm{L}} = n_1$, $n_1 = n_2$, and $n_2 = n_{\mathrm{L}} + \rho(n_{\mathrm{R}} - n_{\mathrm{L}})$
  end if
while $|n_2 - n_1| > t_{\mathrm{tol}}$
Output: Optimal pilot length $n_{\mathrm{p}}^{*} = \arg\min_{n_{\mathrm{p}}} \epsilon_m(n_{\mathrm{p}})$ where $n_{\mathrm{p}} \in \{[(n_{\mathrm{L}} + n_{\mathrm{R}})/2], [(n_{\mathrm{L}} + n_{\mathrm{R}})/2] + 1\}$

Table 1. Simulation parameters

Parameters	Values
Amount of transmit antennas N	$[2, 10]$
Amount of APs K	$[100, 800]$
Amount of UE M	$[50, 400]$
Uplink pilot transmit power $\overline{\mathcal{P}}_{\mathrm{p}}$ for each UE	$[1, 10]$ W
Average downlink transmit power $\overline{\mathcal{P}}_{\mathrm{d}}$	$[1, 40]$ W

4 Numerical Results

MATLAB-based simulations are carried out to validate and evaluate our proposed cell-free massive MIMO based schemes for minimizing the error probability in the finite blocklength regime. The simulation parameters are set as Table 1.

In Fig. 2, we set the amount of transmit antennas $N = 4$, the multiplexing order $Q_m = 2$, the uplink pilot transmit power $\overline{\mathcal{P}}_{\mathrm{p}} = 1$ W, and the average downlink transmit power $\overline{\mathcal{P}}_{\mathrm{d}} = 10$ W. The error probability ϵ_m varies within $[10^{-7}, 10^{-5}]$, and the latency t_{D} varies within $[0.1\ \mathrm{ms}, 0.5\ \mathrm{ms}]$. Fig. 2 shows that the achievable data rate $R_m(t_{\mathrm{D}}, m)$ varies with latency t_{D} and error probability ϵ_m. It can be seen from Fig. 2 that when the error probability is given, the achievable data rate is obviously a monotonically increasing function of latency. As the amount of APs increases, the favorable propagation brought by a great quantity of APs can reduce the interference among massive users. Specifically, when the error probability given by 10^5, by increasing the amount of APs form 100 to 200, the achievable data rate can be improved by 9.8%.

In Fig. 3, we set the amount of APs $K = 200$, the amount of UE $M = 100$, the amount of transmit antennas $N = 10$, the multiplexing order $Q_m = 2$, the uplink pilot transmit power $\overline{\mathcal{P}}_{\mathrm{p}} = 1$ W, and the average downlink transmit power

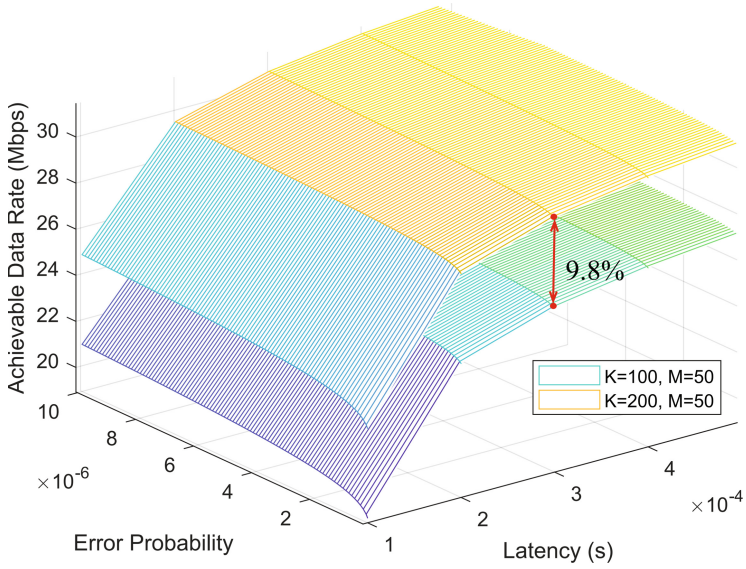

Fig. 2. The achievable data rate $R_m(t_{\mathrm{D}}, \epsilon_m)$ vs. latency t_{D} and error probability ϵ_m in the FBL regime.

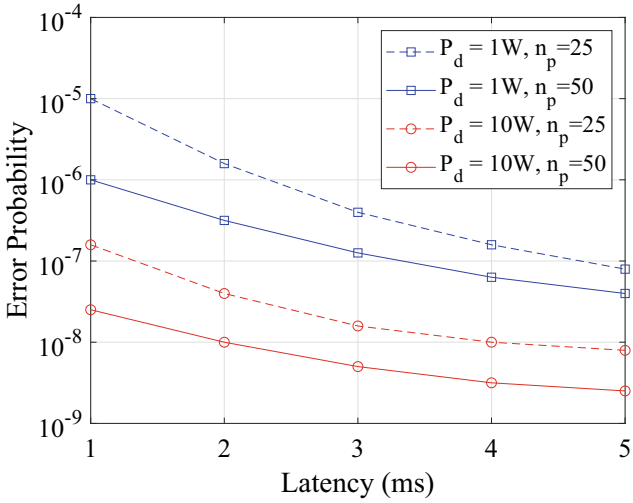

Fig. 3. The error probability ϵ_m vs. latency t_{D} for the proposed cell-free massive MIMO system in the FBL regime.

$\overline{\mathcal{P}}_{\mathrm{d}} = 10$ W. Figure 3 demonstrates the trade-off between error probability and latency. We can see from Fig. 3 that there is a trade-off between error probability and latency over 6G cell-free massive MIMO system in the FBL regime. Therefore, according to the different requirements of 6G applications for latency and reliability, we should reasonably configure the parameters to meet different application requirements. Furthermore, increasing the transmit power of downlink data transmission can effectively reduce the error probability.

In Fig. 4, we set the amount of APs $K = 200$, amount of UE $M = 100$, amount of transmit antennas $N = 8$, the multiplexing order $Q_m = 4$, and the uplink pilot transmit power $\overline{\mathcal{P}}_{\mathrm{p}} = 1$ W. We set the average downlink transmit power $\overline{\mathcal{P}}_{\mathrm{d}} = 1$ or 10 W, respectively. The theoretical value and the simulation value of error probability under different pilot lengths are shown in Fig. 4. As mentioned in the previous analysis, proper pilot length can reduce the error probability. It can be seen from Fig. 4 that the optimal pilot length is 50, which is obtained by the golden section search algorithm. By means of the simulation results, it is found that the theoretical value is consistent with the simulation value, which proves the correctness of the above theoretical analysis. We also find that the optimal pilot length (pentagram) determined by the low complexity golden section search algorithm is consistent with the pilot length (diamond) determined based on the exhaustive search method, which verifies the effectiveness of the golden section search algorithm.

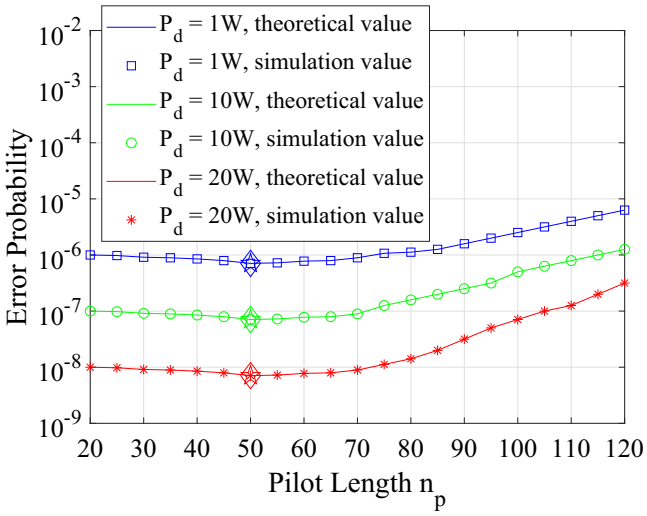

Fig. 4. The error probability ϵ_m vs. pilot length n_{p} in the FBL regime.

In Fig. 5, we set the average downlink transmit power $\overline{\mathcal{P}}_{\mathrm{d}} \in \{1\,\mathrm{W}, 10\,\mathrm{W}\}$, and the multiplexing order $Q_m \in \{2, 4\}$. Figure 5 plots the achievable data rate with varying amount of APs for the proposed 6G cell-free massive MIMO networks.

From Fig. 5, we can find that the achievable data rate increases with the amount of APs. Figure 5 reveals that a larger multiplexing order Q_m can increase the achievable data rate. Figure 5 also demonstrates that the gap between different multiplexing orders increases with the amount of APs, which is the result from the channel hardening effect. We can also find that increasing the multiplexing order Q_m can improve the achievable data rate. Specifically, by increasing the multiplexing order Q_m from 2 to 4, the achievable data rate is improved by up to 6% and 9.9%, respectively.

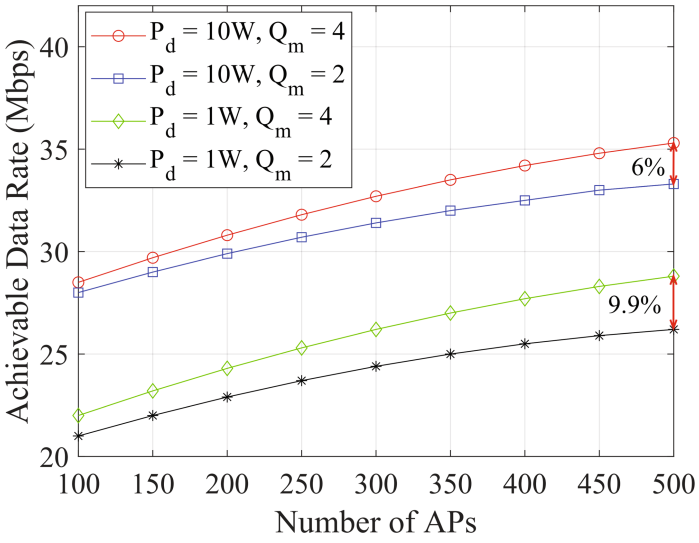

Fig. 5. The achievable data rate vs. amount of APs in the FBL regime.

In Fig. 6, we let the amount of UE $M = 100$, the amount of transmit antennas $N = 10$, the multiplexing order $Q_m = 2$, and the uplink pilot transmit power $\overline{\mathcal{P}}_{\mathrm{p}} = 1$ W. Given different average downlink transmit power and pilot length, Fig. 6 depicts the error probability with varying amounts of APs. Obviously, we can find that the error probability decreases with the amounts of AP increasing. We can see from Fig. 6 that the pilot length n_{p} can make an impact on the error probability, and the proper pilot length can significantly reduce the error probability, which makes the pilot optimization problem more necessary. Specifically, compared with the case where the pilot length is equals to the amount of UE ($n_{\mathrm{p}} = M = 100$), the optimal pilot length can improve the error probability by up to 7.2% and 15.9% when $K = 100$, respectively.

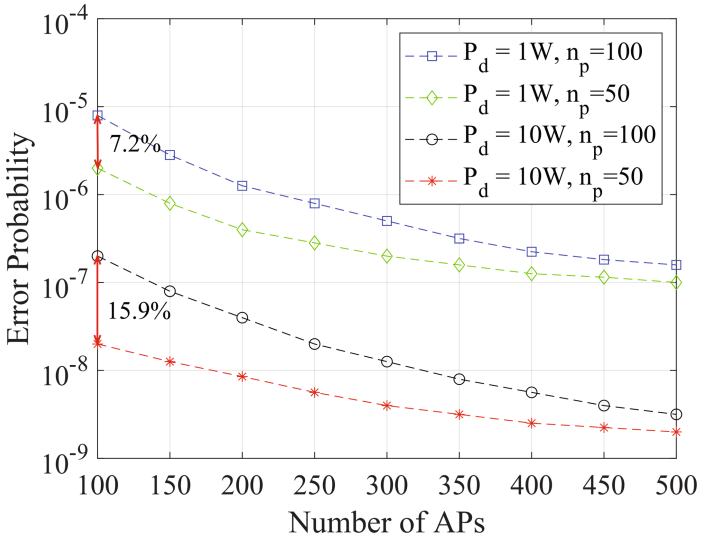

Fig. 6. The error probability vs. amount of APs in the FBL regime.

5 Conclusion

In this paper, we have developed an analytical model and quantitatively characterized the metrics over 6G cell-free massive MIMO mobile wireless networks in the FBL regime. We have derived the SINR for each UE and analyzed the error probability performance in the downlink data transmission. Then, we have formulated the pilot allocation problem with the goal of minimizing the error probability, which has been solved by the golden section search algorithm. A number of simulations have been conducted to verify and evaluate the proposed cell-free massive MIMO scheme in the FBL regime. Our research can effectively meet the requirements for mURLLC in 6G networks, and is of great significance to the theoretical research and actual deployment of cell-free massive MIMO systems.

References

1. Tariq, F., et al.: A speculative study on 6G. Wirel. Commun. **27**(4), 118–125 (2020)
2. Saad, W., Bennis, M., Chen, M.: A vision of 6G wireless systems: applications, trends, technologies, and open research problems. IEEE Netw. **34**(3), 134–142 (2020)
3. Yang, H., et al.: Artificial-intelligence-enabled intelligent 6G networks. IEEE Netw. **34**(6), 272–280 (2020)
4. Matthaiou, M., et al.: The road to 6G: ten physical layer challenges for communications engineers. IEEE Commun. Mag. **59**(1), 64–69 (2021)
5. Bjrnson, E., Sanguinetti, L.: Making cell-free massive MIMO competitive with MMSE processing and centralized implementation. IEEE Trans. Wirel. Commun. **19**(1), 77–90 (2020)

6. Buzzi, S., Andrea, C.D., Zappone, A., Elia, C.D.: User-centric 5G cellular networks: resource allocation and comparison with the cell-free massive MIMO approach. IEEE Trans. Wirel. Commun. **19**(2), 1250–1264 (2020)
7. Ngo, H.Q., Ashikhmin, A., Yang, H., Larsson, E.G., Marzetta, T.L.: Cell-free massive MIMO versus small cells. IEEE Trans. Wirel. Commun. **16**(3), 1834–1850 (2017)
8. Wang, D., et al.: Implementation of a cloud-based cell-free distributed massive MIMO system. IEEE Commun. Mag. **58**(8), 61–67 (2020)
9. Attarifar, M., Abbasfar, A., Lozano, A.: Random vs structured pilot assignment in cell-free massive MIMO wireless networks. In: 2018 IEEE International Conference on Communications Workshops (ICC Workshops), Kansas City, MO, USA, pp. 1–6 (2018)
10. Sabbagh, R., Pan, C., Wang, J.: Pilot allocation and sum-rate analysis in cell-free massive MIMO systems. In: 2018 IEEE International Conference on Communications (ICC), Kansas City, MO, USA, pp. 1–6 (2018)
11. Li, Y., Baduge, G.A.A.: NOMA-aided cell-free massive MIMO systems. IEEE Wirel. Commun. Lett. **7**(6), 950–953 (2018)
12. Bashar, M., Cumanan, K., Burr, A. G., Debbah, M., Ngo, H. Q.: Enhanced max-min SINR for uplink cell-free massive MIMO systems. In: 2018 IEEE International Conference on Communications (ICC), Kansas City, MO, USA, pp. 1–6 (2018)
13. Chen, X., et al.: Massive access for 5G and beyond. IEEE J. Sel. Areas Commun. **39**(3), 615–637 (2021)
14. Polyanskiy, Y., Poor, H.V., Verdu, S.: Channel coding rate in the finite blocklength regime. IEEE Trans. Inf. Theory **56**(5), 2307–2359 (2010)
15. Zhang, X., Wang, J., Poor, H.V.: Statistical delay and error-rate bounded QoS provisioning for mURLLC over 6G CF M-MIMO mobile networks in the finite blocklength regime. IEEE J. Sel. Areas Commun. **39**(3), 652–667 (2021)
16. Caire, G., Shamai, S.: On the achievable throughput of a multiantenna Gaussian broadcast channel. IEEE Trans. Inf. Theory **49**(7), 1691–1706 (2003)
17. Hochwald, B.M., Marzetta, T.L., Tarokh, V.: Multiple-antenna channel hardening and its implications for rate feedback and scheduling. IEEE Trans. Inf. Theory **50**(9), 1893–1909 (2004)